Helmholtz-Zentrum Geesthacht
Zentrum für Material- und Küstenforschung

Final Draft
of the original manuscript:

Balk, M.; Behl, M.; Noechel, U.; Lendlein, A.:

Architectured Shape-Memory Hydrogels with Switching Segments Based on Oligo(Epsilon-caprolactone)

In: MRS Advances (2016) Cambridge University Press

DOI: 10.1557/adv.2016.414

Architectured Shape-Memory Hydrogels with Switching Segments Based on Oligo(ε-caprolactone)

Maria Balk[1,2], Marc Behl[1,2], Ulrich Nöchel[1], and Andreas Lendlein[1,2,3]
[1]Institute of Biomaterial Science, Helmholtz-Zentrum Geesthacht, Teltow, Germany
[2]Tianjin University - Helmholtz-Zentrum Geesthacht, Joint Laboratory for Biomaterials and Regenerative Medicine, Teltow, Germany
[3]Berlin-Brandenburg Center for Regenerative Therapies (BCRT), Teltow, Germany

ABSTRACT

Shape-memory hydrogels (SMHs) are potential candidate materials for biomedical applications as they can mimic the elastic properties of soft tissue and exhibit shape transformations at body temperature. Here we explored, whether architectured SMHs can be designed by incorporating oligo(ε-caprolactone) (OCL, $\overline{M}_n$ = 4500 g·mol^{-1}, T_m = 54 °C) side chains as switching segment into hydrophilic polymer networks based on *N*-vinylpyrrolidone as backbone forming component and oligo(ethylene glycol)divinylether (OEGDVE, $\overline{M}_n$ = 250 g·mol^{-1}) as crosslinker. By utilizing NaCl and $NaHCO_3$ as porogene during thermal crosslinking architectured hydrogels having pore diameters between 30 and 500 µm and wall thicknesses ranging from 10 to 190 µm in the swollen state were synthesized. According to the porous microstructure, a macroscopic form stability was obtained when the polymer networks were swollen until equilibrium in water. Material properties were investigated as function of the OCL content, which was varied between 20 and 40 wt%. In compression experiments the architectured hydrogels exhibited strain fixity and strain recovery ratios above 80%. These architectured SMHs might enable biomaterial applications as smart implants with the recovery of bulky structures from compact shapes.

INTRODUCTION

Thermally-induced SMHs were achieved by crosslinking of hydrophilic segments allowing the swelling in water and hydrophobic side chains, which provide temporary netpoints as switching domains by crystallization to enable the directed movement of the material [1-3]. This research is motivated by a demand for soft shape-memory polymers for minimally invasive surgery. However, the reported SMHs were non-porous, would change their outer dimensions during the swelling process, and would show a marginal compressibility. It was postulated that architectured SMHs providing a high porosity would facilitate form stability on the macroscopic level, i.e. reduction of volume expansion after swelling, and would enable a high deformability in compression in comparison to non-porous hydrogels.

Here we explored, whether the introduction of a porous structure on the microscale into SMHs could be created, which enables large deformations in compression and the form stability of the outer dimensions. In the following we present the synthesis of architectured hydrogels, characterize the porous morphology, thermal, thermo-mechanical, and shape-memory properties, and investigate the influence of the switching segment content on these properties/functions.

EXPERIMENTAL PART

Materials

If not otherwise mentioned, chemicals were obtained from Merck (Darmstadt, Germany). The *ε*-caprolactone (CL), 1-hexanol, dibutyltin oxide (DBTO), 2-isocyanatoethyl methacrylate (IEMA), dibutyltin dilaurate (DBTL), *N*-vinyl pyrrolidone (NVP), oligo(ethylene glycol) divinyl ether (OEGDVE) (all Aldrich, Taufkirchen, Germany), sodium chloride, and sodium bicarbonate were used as received. 2,2′-Azobis(2-methylpropionitrile) (AIBN) was recrystallized from ethanol before use. Tetrahydrofuran (THF), methanol, diethyl ether, and hexane were purified by distillation. Dichloromethane (DCM) was purified and dried by distillation over calcium chloride.

Synthesis

Synthesis of OCL-OH: Under an argon atmosphere 694 mmol CL were melted at 130 °C in a Schlenk flask, 16 mmol 1-hexanol and 0.7 mmol DBTO were added, and the reaction mixture was stirred at 130 °C for 7 h. Afterwards the reaction product was dissolved in DCM, precipitated from cold hexane, filtered off, washed with cold hexane, and dried under vacuum until constant weight was achieved.

$\bar{M}_n$ of OCL-OH was calculated by means of ^{1}H-NMR according to equation 1 by the integral peak area of the CH_3 group from the initiator (I_{ini}) at 0.89 ppm, the CH_2 group of the OCL (I_{OCL}) at 4.06 ppm, and the molecular weights of *ε*-caprolactone (M_{CL}) and the initiator (M_{ini}).

$$\bar{M}_n = \frac{I_{OCL}}{I_{ini}} \cdot \frac{3}{2} \cdot M_{CL} + M_{ini} \quad (1)$$

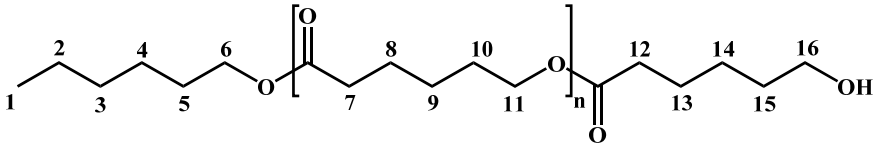

^{1}H-NMR (500 MHz, $CDCl_3$): δ [ppm] = 4.06 (t, ^{3}J(H,H) = 7 Hz, 88H, CH_2-6 and11); 3.65 (t, ^{3}J(H,H) = 7 Hz, 2H, CH_2-16); 2.30 (t, ^{3}J(H,H) = 10.5 Hz, 86H, CH_2-12 and 7); 1.65 (m, 174H, CH_2-5, 8, 10, 13, and 15); 1.38 (m, 92H, CH_2-2, 3, 4, 9, and 14); 0.89 (t, ^{3}J(H,H) = 7 Hz, 3H, CH_3-1).

Synthesis of OCL-IEMA: In a Schlenk flask 11 mmol OCL-OH were dissolved at room temperature under argon atmosphere in 250 mL DCM and 14 mmol IEMA and 0.03 mmol of DBTL were added under intensive stirring [3]. The reaction mixture was further stirred for 5 days. Afterwards the product OCL-MA was precipitated from hexane/diethyl ether/methanol (18/1/1 vol%), filtered off, and dried under vacuum until constant weight was achieved.

The degree of end group functionalization (f_{eg}) with IEMA was calculated by means of ^{1}H-NMR according to equation 2 by the ratio between the integral peak areas of the CH groups of the methacrylate (I_{MA}) (6.12 and 5.59 ppm) and the CH_3 group from the initiator at 0.89 ppm.

$$f_{eg} = \frac{I_{MA}}{I_{ini}} \cdot \frac{3}{2} \cdot 100 \quad (2)$$

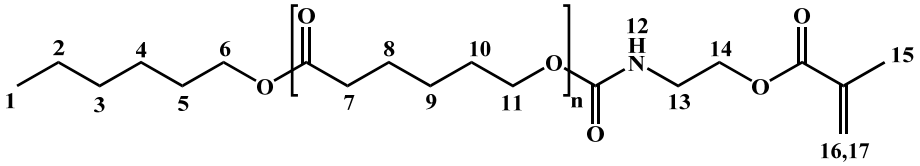

^{1}H-NMR (500 MHz, $CDCl_3$): δ [ppm] = 6.12 (d, ^{3}J(H,H) = 5.5 Hz, 1H, CH-16); 5.59 (d, ^{3}J(H,H) = 5.5 Hz, 1H, CH-17); 4.91 (s, 1H, NH-12); 4.22 (t, ^{3}J(H,H) = 5.5 Hz, 2H, CH_2-14); 4.06 (t, ^{3}J(H,H) = 7 Hz, 88H, CH_2-6 and 11); 3.49 (d, ^{3}J(H,H) = 5.5 Hz, 2H, CH_2-13); 2.30 (t, ^{3}J(H,H) = 10.5 Hz, 86H, CH_2-7); 1.95 (s, 3H, CH_3-15) 1.64 (m, 174H, CH_2-5, 8, and 10); 1.38 (m, 92H, CH_2-2, 3, 4, and 9); 0.89 (t, ^{3}J(H,H) = 7 Hz, 3H, CH_3-1).

Synthesis of architectured hydrogels: OCL-IEMA (20 – 40 wt% in relation to NVP), NVP, 0.75 mol% of OEGDVE (in relation to OCL-IEMA and NVP) were heated to 60 °C under stirring until a homogeneous mixture was obtained. AIBN and the porogenes ($NaCl:NaHCO_3$ = 1:1; $m_{comonomers} = m_{porogenes}$) were added under stirring to the reaction mixture and the thermally crosslinking was performed without stirring at 75 °C for 22 h. The polymer networks were extracted with THF, the salt porogenes were removed with distilled water, and architectured hydrogels were obtained after swelling to equilibrium in water.

Characterization Methods

$\bar{M}_n$ of the precursors were determined for two times on a multidetector GPC consisting of a precolumn, two 300 *x* 0.8 mm M columns (Polymer Standards Service GmbH, Mainz, Germany), an isocratic pump 2080, an automatic injector AS 2050 (both Jasco, Tokyo, Japan), a RI detector Shodex RI-101 (Showa Denko, München, Germany), and a dual detector T60A (Viscotek Corporation, Houston, USA) using chloroform (0.2 wt% toluene as internal standard, 35 °C, 1.0 mL·min^{-1}) as eluent.

The number of hydroxyl end groups was determined by potentiometric titration with a Tritrino 716 (DMS, Metrohm, Filderstadt, Germany).

^{1}H-NMR spectra were recorded at 25 °C in $CDCl_3$ with a Bruker Avance 500 spectrometer (500 MHz, Bruker, Karlsruhe, Germany) with a relaxation time of 2 seconds.

The volumetric degree of swelling Q_v in water was calculated according to reference [4] by the mass of the hydrogel in the dry and in the wet state after removing the water from the hydrogel surface and from the pores by carefully blotting with filter paper.

The form stability of the architectured hydrogels was analyzed by determining the volume of the polymer network in the dry state and after swelling in water until equilibrium.

Differential scanning calorimetry (DSC) experiments were performed on a Netzsch DSC 204 Phoenix (Netzsch, Selb, Germany) in the temperature range between 0 °C and 100 °C with heating and cooling rates of 10 K·min^{-1} in sealed aluminium pans. Thermal properties were determined from the second heating run.

The pore morphology was investigated by light microscopy (Axio Imager.A1m, Carl Zeiss Microimaging, Göttingen, Germany) on glass slides. 20 µm slices were prepared with a microtom of samples in the swelling equilibrium in water. Samples were analyzed in the swollen state in water and after drying on the glass slides. In addition, for scanning electron microscopy

(SEM) measurements freeze-dried samples were cut using sharp razor blades and fixed on holders by conductive adhesive. Samples were sputtered with gold reaching a thickness of 5 nm and afterwards samples were investigated with a desktop-SEM Phenom G2 from PhenomWorld (LOT-Oriel Group Europe, Darmstadt, Germany).

Thermo-mechanical properties were investigated by shear oscillation measurements on a Haake Rheowin Mars II (Thermo Scientific, Karlsruhe, Germany) using a plate-plate geometry. Measurements were carried out in a temperature range between 10 and 65 °C with heating rates of 5 $K \cdot min^{-1}$. Oscillation measurements were performed with a constant amplitude of 4 Pa, a constant frequency of 1 Hz, and with distilled water.

Shape-memory experiments were performed in compression mode on a Haake Rheowin Mars II (Thermo Scientific, Karlsruhe, Germany), whereby the round specimen was compressed at 65 °C to 70%, and cooled to 5 °C under constant strain. Afterwards the stress was released resulting in the temporary shape and the hydrogels were heated to 65 °C under stress free conditions. The specimen was placed in water during shape-memory experiments to enable the reuptake of water during shape recovery.

If not otherwise mentioned, data were given as mean values ± standard deviation of at least three data points and were calculated according to equation 3 and 4, where x is the mean value, N is the number of data points, x_i is the value of the i^{th} measurement, and s is the standard deviation.

$$x = \frac{1}{N}\sum_{i=1}^{N} x_i \tag{3}$$

$$s = \sqrt{\frac{1}{N\text{-}1}\sum_{i=1}^{N}(x_i - x)^2} \tag{4}$$

DISCUSSION

Synthesis of Monofunctionalized OCL and Architectured Hydrogels

The monofunctionalized OCL-OH was synthesized by ring-opening polymerization of CL and initiation with 1-hexanol. A number average of molecular weight ($\bar{M}_n$) of 4500 $g \cdot mol^{-1}$ was detected by end group titration of the terminal hydroxyl groups, and $\bar{M}_n$ was confirmed by GPC and ^{1}H-NMR. The subsequent functionalization of the hydroxyl groups with 2-isocyanato ethylmethacrylate (IEMA) yielded OCL-IEMA having a melting temperature (T_m) of 54±1 °C with a degree of methacrylation of 95% (as determined by ^{1}H-NMR).

Random copolymer networks were synthesized by thermally-induced free radical polymerization of OCL-IEMA providing crystallizable side chains, OEGDVE as hydrophilic crosslinker, and NVP as monomer to build up a hydrophilic backbone in the presence of NaCl and $NaHCO_3$ as pore builders. While NaCl crystals generate cuboid-like pores, $NaHCO_3$ can be pyrolyzed to Na_2CO_3, H_2O, and CO_2, which induces the formation of round pores and facilitates the interconnectivity of pores. Architectured hydrogels were obtained when the pore builders were extracted and the polymer networks were swollen until equilibrium state in water. A series of architectured hydrogels named OCL(x)NVP were synthesized, in which the OCL content x was varied between 20 and 40 wt%.

Characterization of Pore Morphology and Swelling Behavior

The pore morphology was investigated by light microscopy and SEM (figure 1). The architectured hydrogels exhibited heterogeneous pore geometries of cuboid-like and round pores in the swollen as well as in the dry state. Pore diameters ranged from 30 to 500 µm and wall thicknesses between 10 and 190 µm were detected, which were almost independent of the OCL content. The change in wall thickness (Δd_{wall}) between the dry and swollen state was calculated in order to investigate the influence of the side chain content on the swellability of the polymer network (table 1). Δd_{wall} decreased with increasing wt% of OCL from 220 to 150%, which was attributed to the increasing content of hydrophobic OCL domains. In addition, the architectured polymer networks possessed interconnected pores.

Furthermore, the volumes of the samples were determined in the dry and wet state to analyze, if the swelling of the polymer walls can enable the form stability on the macroscopic scale. Therefore, the volumetric expansion (v_{ex}) of the outer dimensions was investigated when the samples were swollen until equilibrium (table 1). v_{ex} decreased from 15±5% to 8±3% with increasing OCL content, which was related to the increasing content of hydrophobic OCL domains. As this expansion was low, the stability of the outer dimensions was maintained.

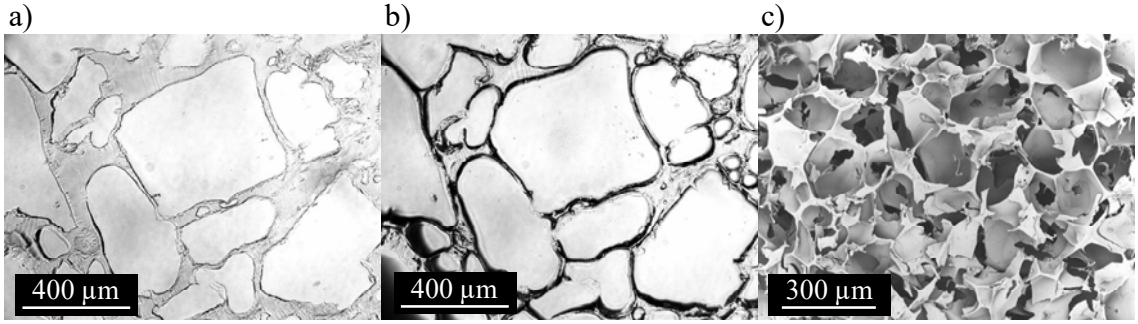

Figure 1. Investigation of the porous morphology of architectured polymer networks. a) Light microscopy of OCL(30)NVP in the swollen state in water and b) in the dry state.c) SEM image of OCL(30)NVP in the freeze-dried state.

The swelling of the networks was investigated by determining Q_v above and below the melting transition of the OCL domains (table 1). According to the definition [5], all polymer networks could be considered as hydrogels as $Q_v \geq 900$ vol%. Q_v decreased as a function of the OCL content from 1600 vol% for OCL(20)NVP to 900 vol% for OCL(40)NVP at 25 °C as a result of the increased hydrophobic character of the polymer networks due to the increased OCL content. Here, Q_v was not affected by the temperature indicating the formation of segregated domains, which prevent the additional uptake of water above T_m due to their hydrophobic character in the semi-crystalline as well as in the amorphous state.

Thermal and Thermo-Mechanical Properties

Thermal properties of OCL(x)NVP hydrogels were studied by means of DSC in the swelling equilibrium in water in a temperature range between 0 and 100 °C. The T_ms (in the second heating run) were independent from the OCL content and were obtained between 48±2 °C and 49±2 °C (table 1). While the uncrosslinked OCL-IEMA exhibited a melting

transition of about 54±1 °C, the crosslinking reaction depressed T_m as result of the sterical hindrance of OCL side chain crystallization in the polymer network architecture.

Shear oscillation measurements were performed on the series of architectured hydrogels at $T < T_m$ (25 °C) and at $T > T_m$ (65 °C). Here, the storage modulus (G') was detected to compare the mechanical properties of the swollen networks within the series of hydrogels in the semi-crystalline as well as in the amorphous state (table 1). Below the melting transition, G' decreased as a function of the OCL fraction from 20 ± 10 kPa for OCL(20)NVP to 190 ± 30 kPa for an OCL content of 40 wt%, which was related to the increasing number of physical crosslinks. When the architectured hydrogels were heated to $T > T_m$, the stiffness of the material decreased to $G' \leq 5 \pm 1$ kPa due to the dissolution of OCL crystals. Therefore, at 65 °C only covalent crosslinks contributed to G'.

Table1. Change in wall thickness (Δd_{wall}) between dry and swollen state, volumetric expansion (v_{ex}) after swelling, volumetric degree of swelling in water (Q_v) at 25 and 65 °C, melting temperature (T_m), shear modulus (G') at 25 and 65 °C, strain fixity (R_f) and strain recovery (R_r) ratios of architectured OCL(x)NVP hydrogels.

Sample-ID	Δd_{wall} [%]	v_{ex} [%]	$Q_{v,\,25\,°C}$ [vol%]	$Q_{v,\,65\,°C}$ [vol%]	T_m [°C]	$G'_{25\,°C}$ [kPa]	$G'_{65\,°C}$ [kPa]	R_f [%]	R_r [%]
OCL(20)NVP	220 ± 50	15 ± 5	1600 ± 100	1700 ± 100	48 ± 2	20 ± 10	1 ± 1	82 ± 3	94 ± 4
OCL(25)NVP	190 ± 50	15 ± 4	1500 ± 200	1400 ± 200	48 ± 2	110 ± 10	3 ± 1	85 ± 4	95 ± 3
OCL(30)NVP	170 ± 20	14 ± 3	1400 ± 100	1500 ± 100	49 ± 2	120 ± 30	3 ± 1	87 ± 4	94 ± 5
OCL(35)NVP	160 ± 30	10 ± 4	1000 ± 100	1000 ± 100	48 ± 2	140 ± 40	5 ± 1	88 ± 3	96 ± 4
OCL(40)NVP	150 ± 10	8 ± 3	900 ± 100	900 ± 100	48 ± 2	190 ± 30	5 ± 1	95 ± 3	95 ± 5

Shape-Memory Properties

The shape-memory properties of architectured OCL(x)NVP hydrogels were investigated by thermo-mechanical compression tests according to descripted methods for non-swollen porous shape-memory polymers [6] from which the strain fixity (Rf) and strain recovery (Rr) ratios were calculated [3]. The measurements consisted of a deformation, fixation, and recovery step as shown for OCL(30)NVP in figure 2. The architectured hydrogel in the permanent shape (figure 2a) was heated to 65 °C, whereby the OCL switching domains became amorphous. Afterwards, the sample was deformed by 70% of compression (figure 2b). This shape was fixed by cooling to 5 °C facilitating the formation of temporary netpoints caused by the recrystallization of OCL side chains and was obtained when the stress was released (figure 2c).

Subsequently, the thermally triggered recovery of the permanent shape (figure 2d) was achieved by heating above the melting transition of the OCL switching domains. The synthesized architectured hydrogels exhibited good R_f-values (table 1), which increased with increasing OCL content from 82 ± 3% for OCL(20)NVP to 95 ± 3% for OCL(40)NVP, which was attributed to an increase in temporary netpoints enabling the stabilization of the temporary shape. The permanent shape was almost completely recovered with R_rs > 94 ± 4%, which were independent on the wt% of the switching segment. Furthermore, the switching temperature (T_{sw}) was determined by the derivative of the compression versus temperature curve. A T_{sw} = 51±3 °C was detected for the series of architecture hydrogels, which was not influenced by the OCL content.

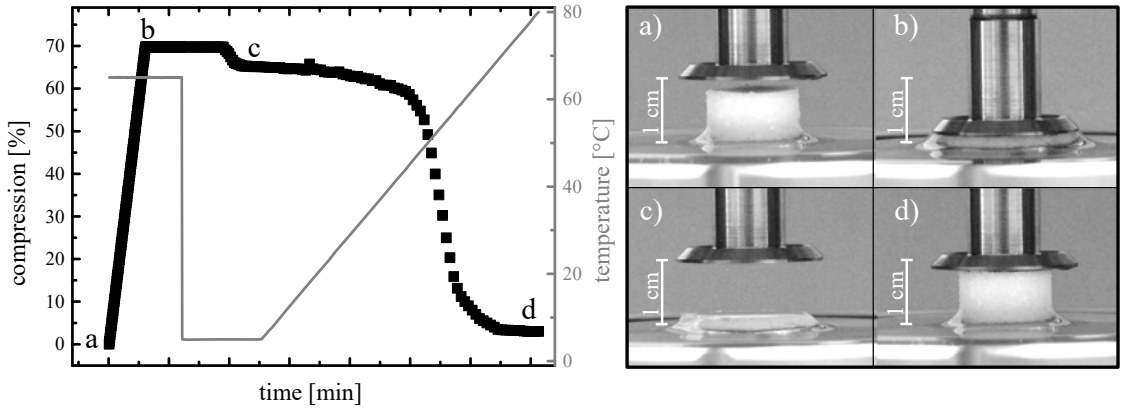

Figure 2. Shape-memory effect in compression mode of architectured hydrogels. OCL(30)NVP in the permanent shape (a) was compressed to 70% at 65 °C (b). The temporary shape (c) was fixed by cooling to 5 °C and was preserved when the stress was released. The recovery was initiated by heating above T_m of the OCL switching domain resulting in the recovered shape (d).

CONCLUSIONS

Architectured SMHs having crystallizable OCL side chains as switching domains could be created by thermal crosslinking of monofunctionalized OCL-IEMA (weight fractions between 20 and 40 wt%), NVP forming a hydrophilic backbone, and OEGDVE as crosslinker in the presence of NaCl and $NaHCO_3$ as porogenes. The incorporated porogenes formed cuboid-like and round pores with diameters from 30 to 500 µm and wall thicknesses between 10 to 190 µm. While the swelling in water induced an increase in polymer wall thickness on the microscopic scale, the overall volume on the macroscopic level was almost unaffected whereby the shape stability was obtained. The degree of swelling decreased with increasing OCL content and was almost independent of temperature. T_m was not affected by the wt% of OCL, whereas G' increased within the kPa range with increasing fraction of the switching segment. All synthesized architectured hydrogels were capable of a shape-memory effect, when a compression of up to 70% was applied and provided R_f- and R_r-values above 80% upon expansion. In conclusion, these architectured SMHs might be suitable for biomedical applications where the recovery of voluminous structures from small, compact shapes are important factors, e.g. for smart implants.

REFERENCES

1. Y. Osada, A. Matsuda, *Nature* **376**, 219 (1995).
2. A. Matsuda, J. i. Sato, H. Yasunaga, Y. Osada, *Macromolecules* **27**, 7695 (1994).
3. M. Balk, M. Behl, U. Nöchel, A. Lendlein, *Macromol. Mater. Eng.* **297**, 1184 (2012).
4. W. Wagermaier, K. Kratz, M. Heuchel, A. Lendlein, *Adv. Polym. Sci.* **226**, 97 (2010).
5. A. S. Hoffman, *Adv. Drug Deliv. Rev.* **54**, 3 (2002).
6. M. A. Di Prima, K. Gall, D. L. McDowell, R. Guldberg, A. Lin, T. Sanderson, D. Campbell,S. C. Arzberger, Mech. Mater. **42**, 405 (2010).